12-1-2009

Influence of Grain Boundary Character on Creep Void Formation in Alloy 617

Thomas Lillo
Idaho National Laboratory

James Cole
Idaho National Laboratory

Megan Frary
Boise State University

Scott Schlegel
Boise State University

INFLUENCE OF GRAIN BOUNDARY CHARACTER ON CREEP VOID FORMATION IN ALLOY 617

Thomas Lillo[1], James Cole[1], Megan Frary[2], Scott Schlegel[2]

[1]Idaho National Laboratory, P.O. Box 1625, Idaho Falls ,ID 83415

[2]Materials Science and Engineering, Boise State University, Boise, ID 83725-2075.

ABSTRACT

Alloy 617, a high temperature creep-resistant, nickel-based alloy, is being considered for the primary heat exchanger for the Next Generation Nuclear Plant (NGNP) which will operate at temperatures exceeding 760°C. Orientation imaging microscopy (OIM) is used to characterize the grain boundaries in the vicinity of creep voids that develop during high temperature creep tests (800-1000°C at creep stresses ranging from 20-85 MPa) terminated at creep strains ranging from 5-40%. Observations using optical microscopy indicate creep rate does not significantly influence the creep void fraction at a given creep strain. Preliminary analysis of the OIM data indicates voids tend to form on grain boundaries parallel, perpendicular or 45° to the tensile axis, while few voids are found at intermediate inclinations to the tensile axis. Random grain boundaries intersect most voids while CSL-related grain boundaries did not appear to be consistently associated with void development.

1. INTRODUCTION

High temperature heat from the proposed Next Generation Nuclear Plant (NGNP) is envisioned to produce electricity more efficiently than current nuclear power plants. However, this high temperature heat will also be used in the production of hydrogen as well as in other industrial processes, Fig. 1. Conditions in the NGNP are expected to be extremely harsh from a materials point of view. The NGNP reactor outlet temperature falls in the range of 760-1000°C [1]. The heat exchanger that isolates the NGNP from hydrogen production and other industrial processes is of particular concern. Although ceramic materials possess the requisite high temperature strength and creep resistance, ceramic heat exchanger reliability and the propensity for ceramics to fail in a catastrophic manner have prevented their consideration for use in nuclear applications, at least in the near future. Currently, the material being focused on for heat exchanger applications in the NGNP is Inconel 617 (I-617). At elevated temperatures, I-617 exhibits relatively short Stage 2 creep behavior and spends most of its creep life in tertiary creep, Fig. 2. Typically, development of creep voids begins during tertiary creep [2] which impairs continued load carrying capabilities. Therefore it is necessary to investigate creep cavity formation at these high temperatures and assess the influence of microstructure, especially grain boundary character, on the propensity for pore formation. This information may result in grain boundary engineering methodologies to reduce creep void formation and increase the lifetime of high temperature components.

2. EXPERIMENTAL METHODS

Creep specimens, conforming to ASTM Standard E 139-06, were fabricated from an Inconel 617 plate with the composition given in Table 1. The ratio of the gage length (16.6 mm) to the diameter of gage section (4.2 mm) was 4.0. High temperature creep tests were carried out using Applied Test Systems, Lever Arm Tester, Series 2410. The creep temperature was monitored with a Type K thermocouple and controlled to within $\pm 3^{o}$C of the target creep temperature. LVDT transducers were used to monitor creep strain during the test and used to determine when the creep strain had attained a target value at which time the test was terminated. Samples were then cooled from the test temperature under load. The actual creep strain was determined by measuring the increase in sample length after it had cooled to room temperature. A representative creep curve is shown in Fig. 2. The creep rate for all samples was determined at approximately 5% creep strain (in the tertiary creep regime) and was used to comparison purposes.

The gage section was mounted and polished to provide a plane of view parallel to the specimen axis. This allowed analysis along the length of the gage section. Metallographic samples were lightly etched to remove flowed metal that may have obscured small creep cavities. Etching was performed by immersing the sample in concentrated hydrochloric acid for 5-10 seconds, rinsing in methanol and then subsequent immersion in a methanol-1% bromine solution for 15-45 seconds. After etching the samples were rinsed in methanol, then water and finally placed in methanol and ultrasonically cleaned for 30 seconds. Vibratory polishing with 0.05 micron colloidal silica for 30 minutes was the final step in the polishing procedure in preparation for OIM analysis.

Determination of the percentage of creep void area for each sample was carried out using a Zeiss, Observer.Z1M and Zeiss software, AxioVision AxioVs 40, version 4.7.1.0. An area of >50 mm^2 was used in this determination and the average void fraction over this region was reported as a percentage.

Orientation Imaging Microscopy (OIM) was performed on these same samples using a Philips XL20 ESEM and the TSL OIM Analysis package, version 4.6. Inconel 617 is a high temperature alloy that acquires its creep resistance from the precipitation of chromium and molybdenum carbides. The OIM system is capable of collecting both orientation and chemical (via EDS) information simultaneously, allowing the discrimination between the two types of carbides (the crystallographic information of the precipitates was not acquired).

Individual pores were evaluated following OIM data collection for the following information:

- Inclination of pore to tensile axis
- Number of precipitates touching pore
    - Cr ppts
    - Mo ppts
- Number of CSL boundaries that intersect pore
- Number of random boundaries that intersect the pore

A total of 150 pores were analyzed from samples subjected to 19 MPa at 1000°C (samples with creep strain of 8% and 15% were used). Additionally, a creep sample of OFHC copper that had been ECAE processed (2A passes through a 90° ECAE die at room temperature) and tested under creep conditions of 450°C and 14 MPa was also analyzed using OIM for comparison purposes. The same OIM information was collected for this sample except the precipitate information (since no precipitates were present in this material).

3. Results and Discussion

3.1 Influence of Creep Strain and Strain Rate on Creep Cavitation

Table 2 shows the conditions and creep strain at test termination for each sample used in this work. This range of test conditions resulted in creep rates that ranged from 8.5 x 10^{-8} %/second to 2.5 x 10^{-7} %/second. The creep temperatures are on the order of $0.8T_{MP}$. The dominant deformation mechanism is expected to be dislocation creep at the stresses applied in these creep tests [3]. (Dislocation creep can be expected to remain the dominate deformation mechanism in NGNP components even though the stresses will be lower to attain useful component lives on the order of 10+ years. However, other creep mechanisms, such as lattice diffusion, i.e. Nabarro-Herring creep, may become significant and will need to considered in the future.) Creep tests were terminated between creep strain values of 5% and 41%. These conditions were sufficient to produce a significant fraction of creep voids as shown in Fig. 3. Image analysis was capable of detecting creep cavities approaching 1 micron in diameter. The percentage of creep void area as a function of creep strain is plotted in Fig. 4 for the three different load/temperature combinations (and, therefore, three different creep rates). The percentage of creep porosity increases with increasing strain, as expected, however no clear differences between the three different creep rates is discernable. The creep rates differ by less than an order of magnitude and, therefore, the differences may be small – possibly falling within the scatter of the measurements. Furthermore, the distribution of creep porosity is not uniform throughout the gage section – typically being concentrated within a small area. However, plotting the maximum percentage of creep void area found in the gage section as a function of creep strain does not clarify the results, Fig. 5. Alternatively, there has been some work done that implies that the percentage of creep porosity should only be a function of creep strain and not of applied stress (and, therefore, creep rate) [4]. The density of creep cavity nucleation sites is basically constant with applied stress and the growth of creep cavities is controlled by grain boundary sliding. Since grain boundary sliding accommodates the creep strain, the percentage of porosity may be tied to only the creep strain – a reasonable interpretation of the results in Figs. 4 & 5. Additional measurements may be needed to not only improve statistics but to determine if the creep rate, indeed, has little influence on creep void nucleation and growth.

3.2 Influence of Grain Boundary Character on Creep Voids

Orientation Imaging Microscopy (OIM) was used to explore the influence of grain boundary character on the development of creep voids. Grain boundary parameters (misorientation, random versus CSL-related, grain boundary habit plane, etc.) can be expected to influence the density of potential void nucleation

sites, ease of grain boundary sliding and grain boundary diffusion [4,5]. Therefore, a preliminary attempt was made to relate creep void development with grain boundary character.

Figure 6 shows the information that can be obtained from OIM analysis. The forward scattered electron image of a region is shown in Fig. 6a while the image quality of the backscattered electron diffraction patterns, as calculated by the OIM software, is mapped onto the same region in Fig. 6b. The grain boundaries and precipitates are shown in Fig. 6c, where the chromium carbides are red (the molybdenum carbides are not shown), the random grain boundaries are black and the CSL-related grain boundaries are green. An example of the information obtained from a given pore (outlined by the red box in Fig. 6c) is shown in Fig. 7. For this particular pore there are three random grain boundaries that intersect the pore while only one CSL-related boundary intersects the pore (a Σ3, in this case). Two chromium-rich carbides (the small red/pink grains) are associated with the pore (two molybdenum-rich carbides also are associated with the pore but appear white in this photo). The pore is oriented at roughly 35^{o} to the tensile axis of the creep test which is horizontal in the photo.

The precipitates in the I-617 alloy represent an added complication to the interpretation of the data. Therefore, a creep sample of pure copper was also analyzed for comparison purposes and to eliminate the complication introduced by precipitates. The copper creep specimen was taken from a bar that had been subjected to severe plastic deformation (Equal Channel Angular Extrusion at room temperature by 2A passes – deformation strain of approximately 2 prior to creep testing). This material is known to recrystallize at relatively low temperatures and produce a highly twinned microstructure – much like that of I-617. The creep conditions for this sample were 450^{o}C and 14 MPa. Figure 8 shows that the microstructure *after* a creep strain of 3.4% is very similar to that of I-617 in Fig. 6c. The same information was collected in the pores in this material as that of the I-617 samples (except for the precipitate information, of course).

The inclination of pores to the tensile axis is shown in Fig. 9. It would appear that voids are preferentially aligned parallel, perpendicular or 45^{o} to the tensile axis. The results for the copper sample are very close to those for the I-617 except the voids on boundaries parallel to the tensile are not as prevalent as in I-617. Voids on grain boundaries oriented perpendicular to the tensile axis experience the greatest normal force during creep, tending to open up voids. Voids on grain boundaries at 45^{o} to the tensile axis are on planes of maximum shear where grain boundary sliding should be prevalent. The voids on grain boundaries oriented parallel to the tensile axis, however, present somewhat of a mystery as no accepted explanation can be given. Although the different atomic diffusivity of nickel, chromium and molybdenum atoms in the grain boundary may be responsible – perhaps in much the same manner as in the development of Kirkendall porosity in diffusion couples of elements with radically different lattice diffusivity [6]. The lack of substantial amounts of impurity atoms with different grain boundary diffusivity may result in the low number of voids on boundaries parallel to the tensile axis in pure copper.

The character of the grain boundary, namely whether it can be classified as random or CSL-related, was also of interest in this work, mainly from the aspect that it might be possible to perform grain boundary engineering to produce a microstructure more resistant to creep void nucleation. The boundary character of grain boundaries intersecting creep voids is plotted in Fig. 10 where Fig. 10a shows the frequency of 0, 1, 2,….,6 random grain boundaries intersecting the pore while CSL-related boundaries are plotted in Fig. 10b. Most pores have one or more random grain boundaries associate with them – pores without a random grain boundary associated with them are not prevalent. For copper, the effect appears more

pronounced and most pores are associated with 2 or more random grain boundaries. Conversely, the frequency of pores *without* a CSL-related grain boundary intersecting them is similar to pores with 1 or more CSL-related grain boundaries associated with them. A similar trend is seen in the copper sample. Random grain boundaries may have a higher density of void nucleation sights or exhibit greater grain boundary sliding compared to CSL-related grain boundaries. In fact, a more important parameter to evaluate may be the grain boundary plane as it determines the atomic structures within the grain boundary and may be the more important parameter in determining whether a grain boundary is "special" or not [7,8].

Finally, for the I-617 material one might expect that the precipitates might act as efficient void nucleation sites, especially since the precipitates frequently occur in clusters of two or more. The results for each type of carbide in contact with the pore are shown in Fig. 11. It would appear that many creep voids are not associated with any precipitates. However, it must be kept in mind that this is only a planar section through the void and voids may be associated with the voids in the other dimensions. It will be difficult to obtain the 3-D precipitate distribution to definitively make a conclusion on the influence of precipitates on creep void nucleation.

4.0 Summary and Conclusions

Evaluation of the relationship between the percentage of void area in the microstructure of creep specimens of Inconel 617 and the amount of creep strain shows that there is not a strong (possibly non-existent) effect of creep rate on this relationship. However, the imposed creep rate in this work varied by less than an order of magnitude (8.5×10^{-7} to 2.5×10^{-7} %/sec) and the porosity measurements exhibited considerable scatter even though a relatively large area (>50 mm^2) was analyzed and, therefore, the differences may not be discernible. Larger areas need to be analyzed to improve statistics and a wider range of creep rates are also needed to reveal a possible dependence on creep rate.

Microstructural characteristics in the vicinity of creep voids were analyzed by OIM with simultaneous acquisition of chemical information by EDS. In I-617, voids were found to be more prevalent on grain boundaries oriented relatively parallel or perpendicular to the tensile axis as well as at 45^o to the tensile axis. The formation of voids on boundaries parallel to the tensile axis could not be easily rationalized as those on boundaries either perpendicular to the tensile axis, where the maximum normal force would occur, or 45^o to the tensile axis, where grain boundary sliding can be expected to be the greatest. Voids on boundaries parallel to the tensile axis were not as prevalent in the pure copper creep samples.

CSL-related grain boundaries did not seem to factor into void formation, however, most voids were intersected by one or more random grain boundaries. These results were found in creep specimens of pure copper as well as in creep specimens of I-617. Also, precipitates were found to be associated with voids as often as not. However, the 3-dimensional distribution of precipitates was not determined and no conclusion can be drawn from the 2-dimensional information collected in this work.

ACKNOWLEDGEMENTS

Prepared for the U.S. Department of Energy, Office of Nuclear Energy, Under DOE Idaho Operations Office, Contract DE-AC07-05ID14517.

REFERENCES

[1] Wu, Q., Song, H., Swindeman, R., Shingledecker, J. and Vasudevan, V., **Metall. And Materials Trans. A**, vol. 39A, 2008, pp. 2569-2585.

[2] Ralls, K.M., Courtney, T.H. and Wulff, J., **Introduction to Materials Science and Engineering**, John Wiley & Sons, New York, 1976, p. 489.

[3] Dieter, G.E., **Mechanical Metallurgy, 3rd Edition**, McGraw-Hill Book Company, New York, 1986, pp. 449-451.

[4] Evans, H.E., **Mechanisms of Creep Fracture**, Elsevier Applied Science Publishers, New York, 1984, pp. 25-62.

[5] Randle, V., **The Measurement of Grain Boundary Geometry**, Institute of Physics Publishing, Philadelphia, 1993, pp. 2-5.

[6] Reed-Hill, R.E., **Physical Metallurgy Principles, 2nd Edition**, PWS Publishers, 1973, pp. 390-397.

[7] Randle, V. **Scripta Materialia**, vol. 54, 2006, pp. 1011-1015.

[8] Kim, C., Rollet, A.D., Rohrer, G.S., **Scripta Materialia**, vol. 54, 2006, pp. 1005-1009.

Table 1. Composition of I-617

C	Mn	Fe	S	Si	Cu	Cr	Al	Ti	Co	Mo	B	Ni
0.08	0.11	1.69	<0.001	0.12	0.04	21.91	0.96	0.34	11.42	9.78	0.002	Bal.

Table 2. Creep Conditions for I-617

Sample ID	Creep Temperature, ^{o}C	Creep Stress, MPa	Creep Strain, %	Test Duration, hours
A-1000-025-05-1	1000	22.9	7.1	97.0
A-1000-025-25-1	1000	23.0	24.2	150.0
A-1000-025-20-1	1000	22.6	41.4	134.7
A-1000-025-20-2	1000	25.9	23.1	158.5
A-1000-025-15-1	1000	23.8	17.0	115.4
A-1000-019-25-1	1000	19.4	23.6	241.3
A-1000-019-20-1	1000	19.4	20.4	312.2
A-1000-019-15-1	1000	19.4	17.7	333.9
A-1000-019-05-1	1000	19.5	4.9	111.3
A-0900-040-20-1	900	39.1	16.5	650.7
A-0900-040-15-1	900	39.1	12.5	427.6

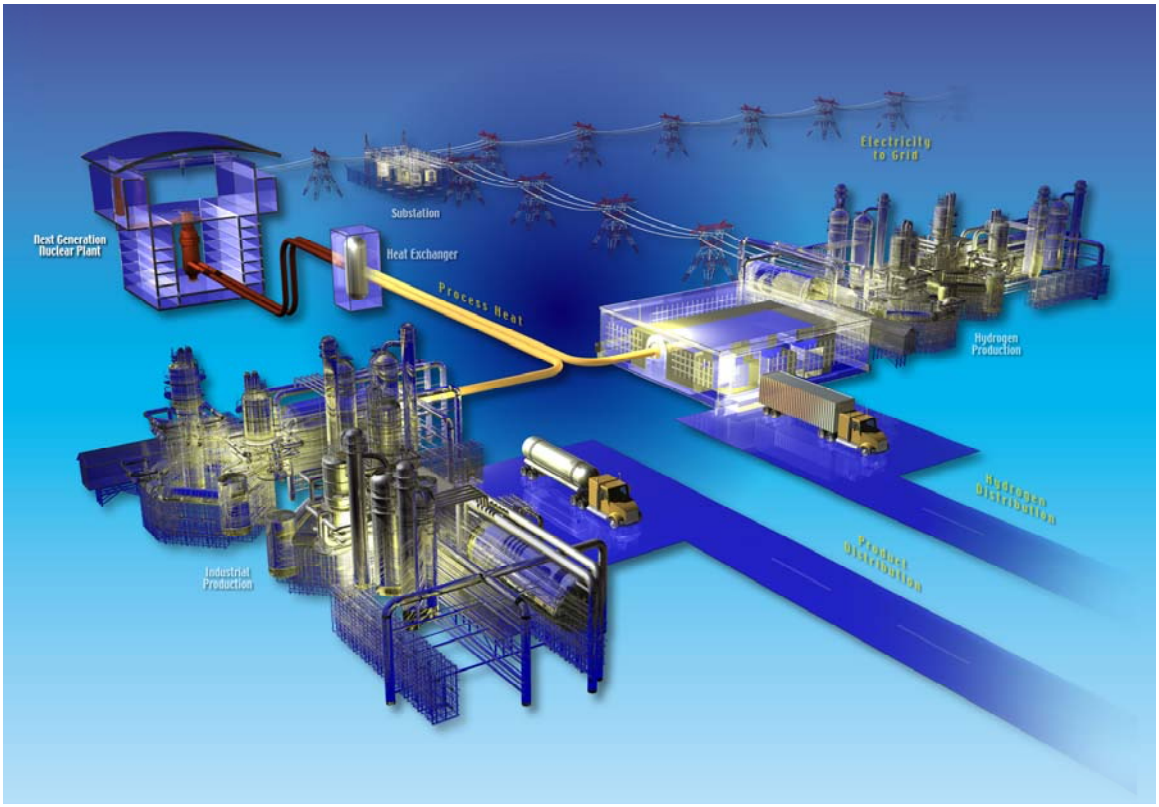

Figure 1. The current concept of the NGNP includes the production of high temperature heat from the nuclear reactor for use in the production of hydrogen and other industrial processes.

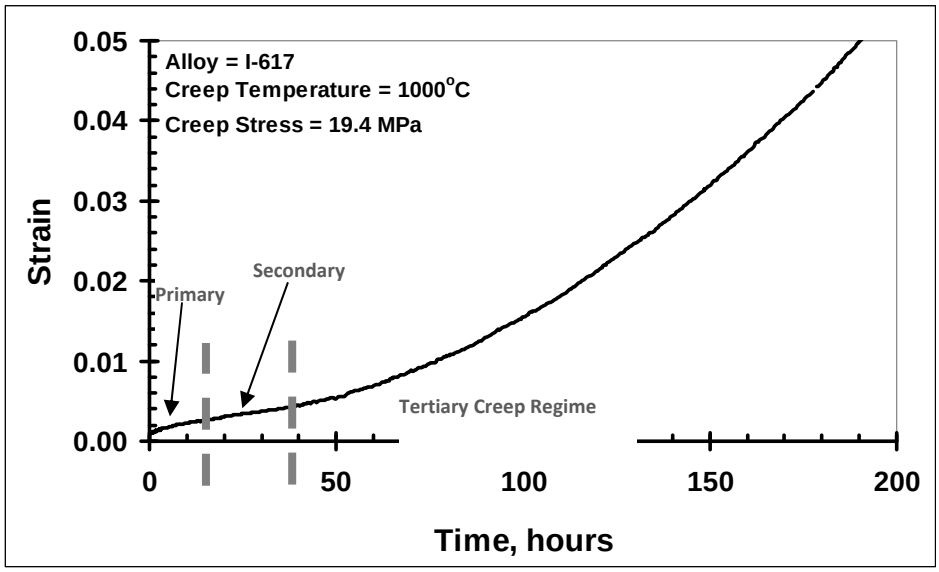

Figure 2. The creep life of I-617 is largely spent in the tertiary creep regime.

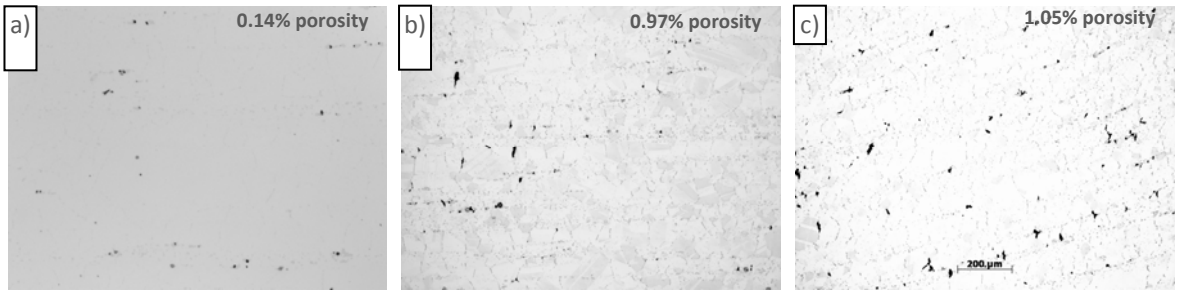

Figure 3. Porosity distribution in I-617 after a creep strain of a) 5%, b) 15% and c) 25%.

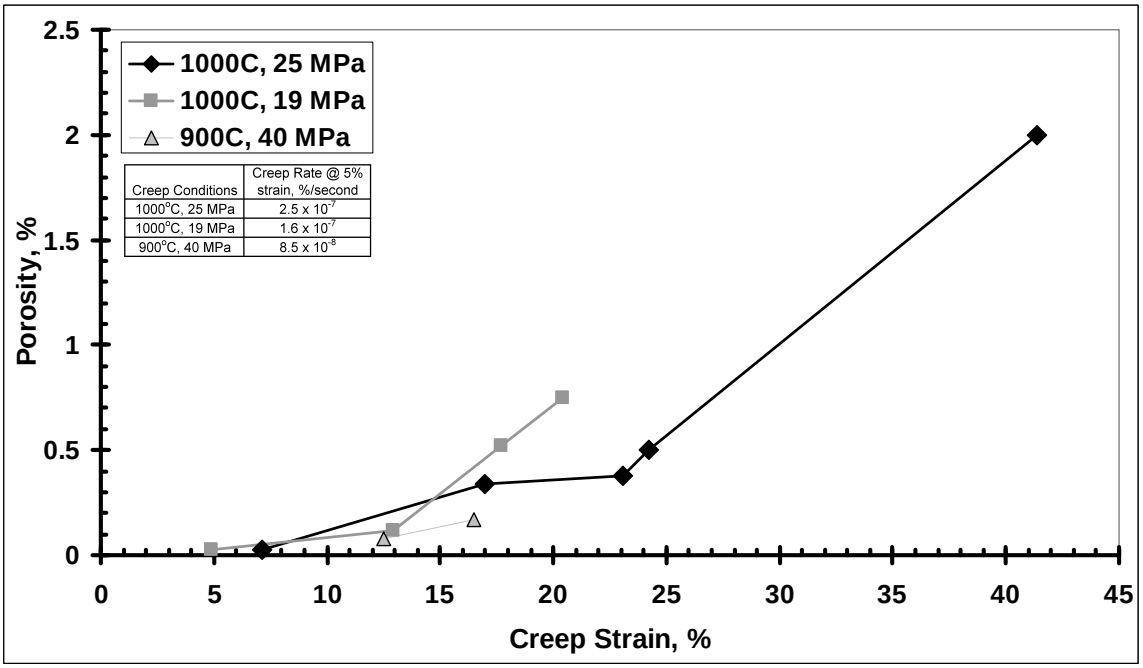

Figure 4. The average fraction of creep void area increases with creep strain. Creep rate does not have a strong influence on this relationship.

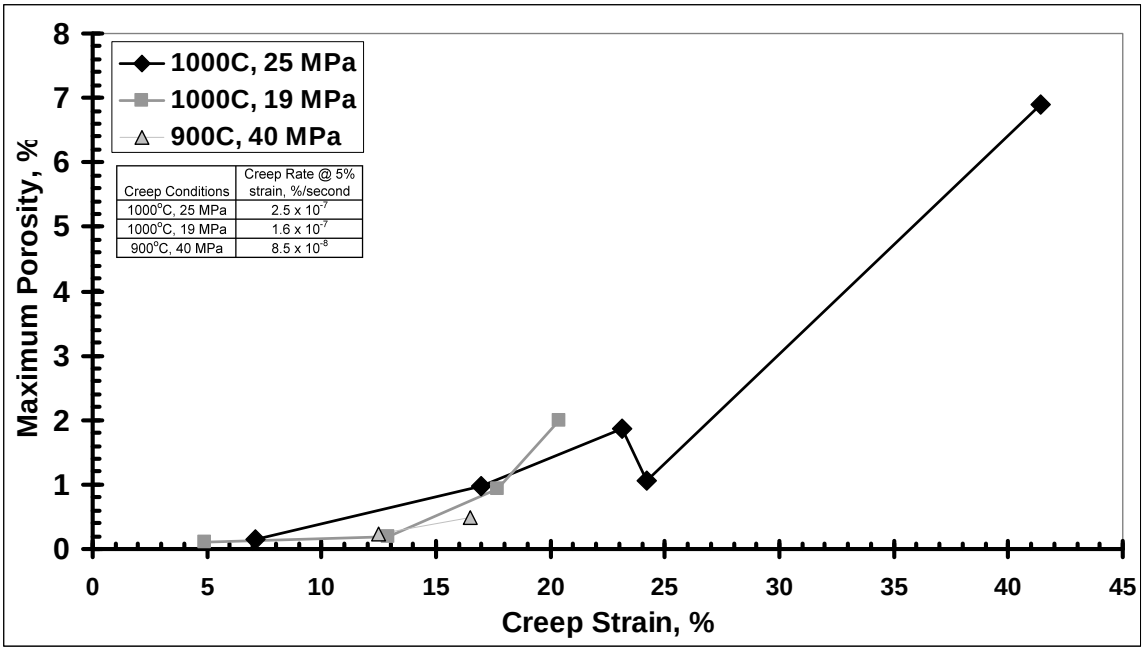

Figure 5. The maximum creep void fraction in the gage section of the creep sample as a function of creep strain also indicates little effect of the imposed creep strain rate.

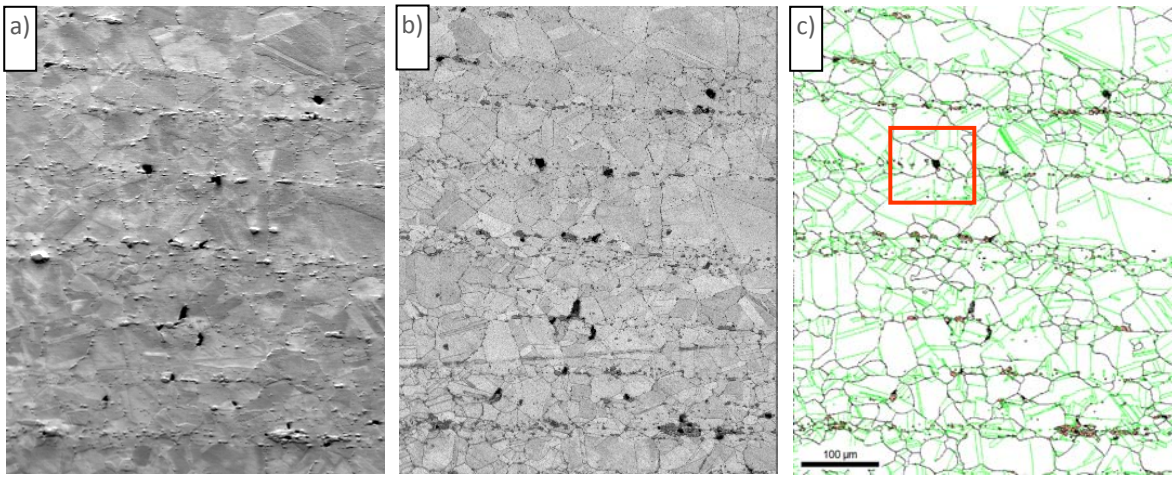

Figure 6. Example of OIM data collection from a given area. A forward scattered electron image in a), the corresponding image quality map in b) and the grain boundary reconstruction in c) where random grain boundaries at black, CSL-related boundaries are green and chromium-rich precipitates are red. Creep voids are black in all images.

- Random grain boundaries are black
- CSL boundaries are green
- Pores are black
- Cr ppts are red

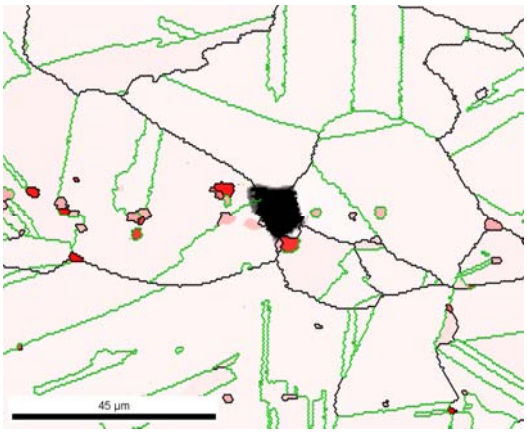

Figure 7. Enlargement of the area in the red box of Fig. 6. Three random and one CSL-related grain boundaries intersect the void, which is oriented at approximately 35° to the tensile axis (horizontal in this image). Two Cr-rich precipitates are in contact with the void (two Mo-rich precipitates are also in contact but are not shown.

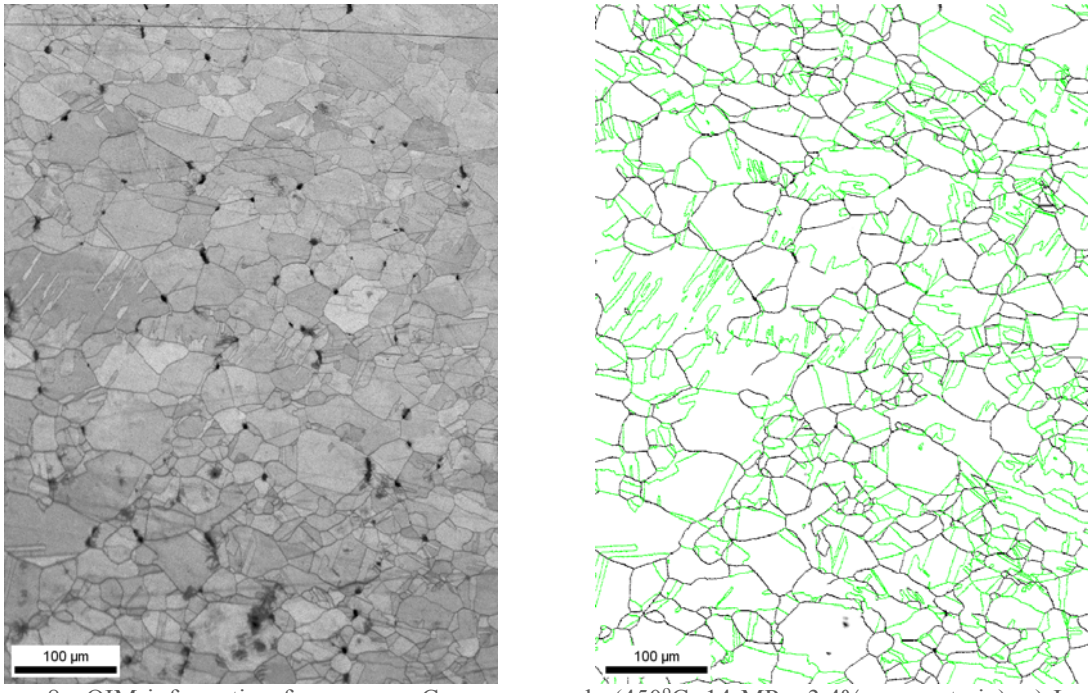

Figure 8. OIM information from a pure Cu creep sample (450°C, 14 MPa, 3.4% creep strain). a) Image quality map and b) grain boundary reconstruction with CSL-related grain boundaries in green and random grain boundaries in black.

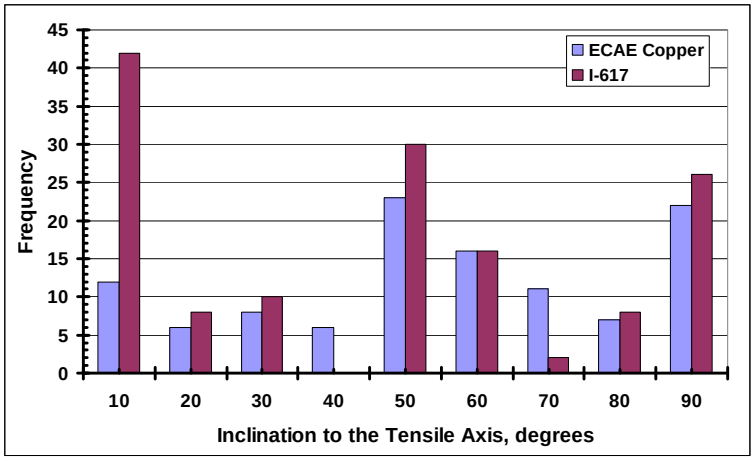

Figure 9. Voids appear to prefer grain boundaries that are perpendicular, 45° or parallel to the tensile axis. Voids on boundaries parallel to the tensile axis are less prevalent in pure Cu than in I-617.

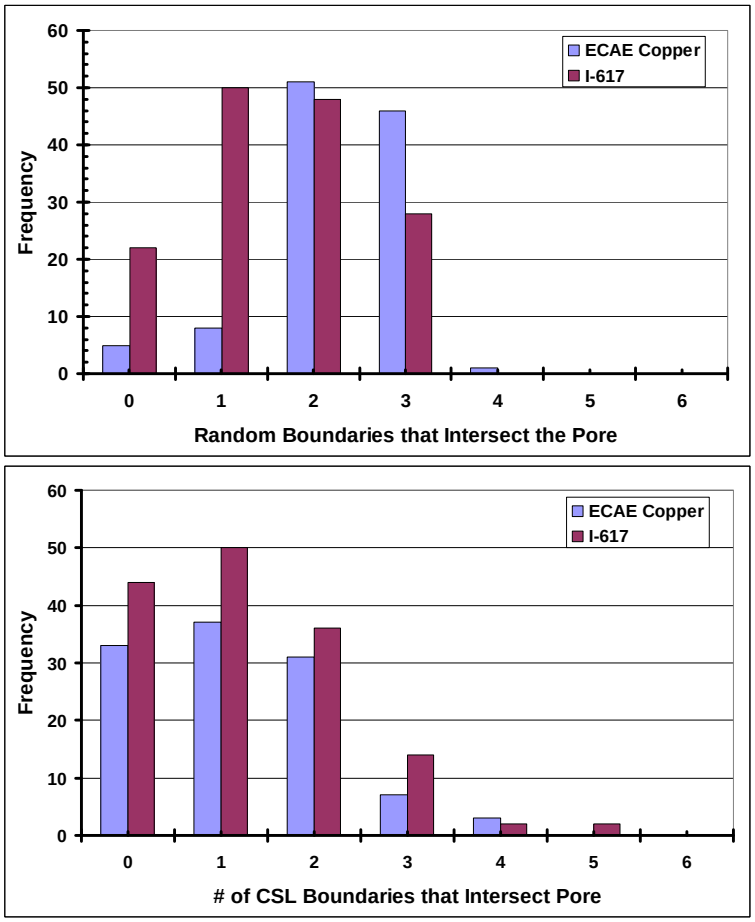

Figure 10. The frequency of a) random and b) CSL-related grain boundaries that intersect voids.

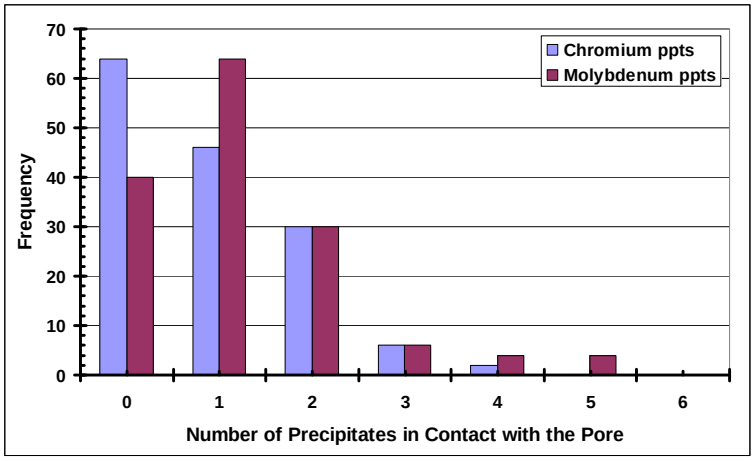

Figure 11. The frequency with which the different precipitate types are associated with voids in I-617.